Journal Name

ARTICLE

Synthesis of Highly Uniform Cu_2O Spheres by a Two-step Approach and their Assembly to Form Photonic Crystals with Brilliant Color

Xin Su,[a] Jie Chang,[a] Suli Wu,*[a] Bingtao Tang[a] and Shufen Zhang[a]

Received 00th January 20xx,
Accepted 00th January 20xx

DOI: 10.1039/x0xx00000x

www.rsc.org/

Monodispersed semiconductor colloidal spheres with high refractive index hold great potential for building photonic crystals with strong band gap, but the difficulty in separating nucleation and growth process make it challenging to prepare highly uniform semiconductor colloidal spheres. Herein, real monodispersed Cu_2O spheres were prepared via a hot-injection & heating-up two-step method using diethyleneglycol as a milder reducing agent. The diameter of as prepared Cu_2O spheres can be tuned from 90 nm to 190 nm precisely. The SEM images reveal that the obtained Cu_2O spheres have narrow size distribution, which permits their self-assembly to form photonic crystal. The effects of precursor concentration and heating rate on the size and morphology of Cu_2O spheres were investigated in detail. The results indicate that the key points of the method include the burst nucleation to form seeds at high temperature followed by rapid cooling to prevent agglomeration, and proper precursor concentration as well as moderate growth rate during the further growth process. Importantly, photonic crystals films exhibiting brilliant structural color were fabricated with the obtained monodispersed Cu_2O spheres as building blocks, proving the possibility of making photonic crystal with strong band gap. The developed method was also successfully applied to prepare monodispersed CdS spheres with diameters in the range from 110 nm to 210 nm.

Introduction

Preparation of monodispersed colloidal spheres with controllable sizes has captured worldwide attention due to their numerous important applications in sensors, ceramics, catalysis and pigments, especially in photonic crystals.[1-4] Most of the colloidal spheres exploited in photonic crystals are mainly focused on polystyrene, polymethyl methacrylate, and silica spheres.[5, 6] However, all these materials have relative low refractive index, which make the photonic crystal has weak band gap and not brilliant structure color.[7, 8] Monodispersed spheres of metal (metal oxide) and semiconductors (ZnO,[9, 10] CdS,[11] ZnS,[7, 12, 13] Pb,[14] Se,[15, 16] TiO_2[17, 18]) are expected to be ideal building blocks for photonic crystals due to their high refractive indices and size-dependent intrinsic properties.

As an important p-type metal oxide semiconductor with a band gap of 2.17 eV, cuprous oxide (Cu_2O) has been widely applied in solar energy conversion,[19] lithium-ion battery anode materials,[20, 21] water splitting,[22] and so on. Because the morphology of Cu_2O has great influence on its optical and catalytic properties, morphology controllable synthesis of Cu_2O has attracted intensive studies.[23-26] It has refractive index of 2.7, which is greatly higher than the case of traditionally used polymer or silica colloidal spheres (1.5-1.6) for building photonic crystal, providing opportunities to realize photonic crystals with strong band gap. In the past decade, a number of efforts have been devoted to prepare Cu_2O spheres. Zeng *et al.*[27] prepared Cu_2O spheres by reducing $Cu(OH)_4^{2-}$ with N_2H_4 in 2-propanol and Wang *et al.*[28] got similar products with water as solvent instead of 2-propanol. Li *et al.*[29] also prepared relatively uniform spheres through reduction of $Cu(CH_3COO)_2$ by $NaBH_4$ in dimethyl formamide. However, the rapid reducing reaction rates of Cu^{2+} make it difficult to separate the nucleation and growth stages and kinetically control these stages separately. Hence, it is essential to slow down the reaction rate by using a relatively milder reducing agent in order to control the process accurately.

Diethyleneglycol (DEG), possessing milder reducing power than the previously used N_2H_4 and $NaBH_4$, has potential to control the nucleation and growth processes of Cu_2O spheres kinetically. The high boiling points of DEG (245 °C) and their highly temperature-dependent reducing power endow them the ability to control growth of Cu_2O over a wide range of temperature.[30] Based on the "two-stage growth model" proposed by Privman and Matijevic for polycrystalline CdS spheres,[31] herein we developed a two-step method to prepare monodispersed Cu_2O spheres using diethyleneglycol (DEG) as reducing agent. The method involves a hot-injection process for seeds formation and a heating-up process for primary particle aggregation-based growth. By separating the two steps and using a milder reducing agent, monodispersed Cu_2O spheres with narrow size distribution are achieved and the particle size can be tuned in the range of 90-190 nm precisely through simply varying the amount of Cu precursor. The formation mechanism of the monodispersed spheres is proposed and the size-dependent optical properties of the obtained spheres are investigated. Based on the developed method, monodispersed CdS spheres with diameters in the range from 110 nm to 210 nm are also prepared. Finally, photonic crystal films with brilliant and saturated structural color are fabricated by self-assembly of monodispersed Cu_2O spheres.

---

[a] *State Key Laboratory of Fine Chemicals, Dalian University of Technology, 2 Linggong Road, Dalian 116024, P.R. China. E-mail: wusuli@dlut.edu.cn*

†Electronic Supplementary Information (ESI) available: Digital images of Cu_2O dispersion in ethanol. Size distribution of Cu_2O spheres in different diameters. SEM images of polydisperse products of reactions for comparison.

Scheme 1. Schematic illustration of the reaction process and mechanism.

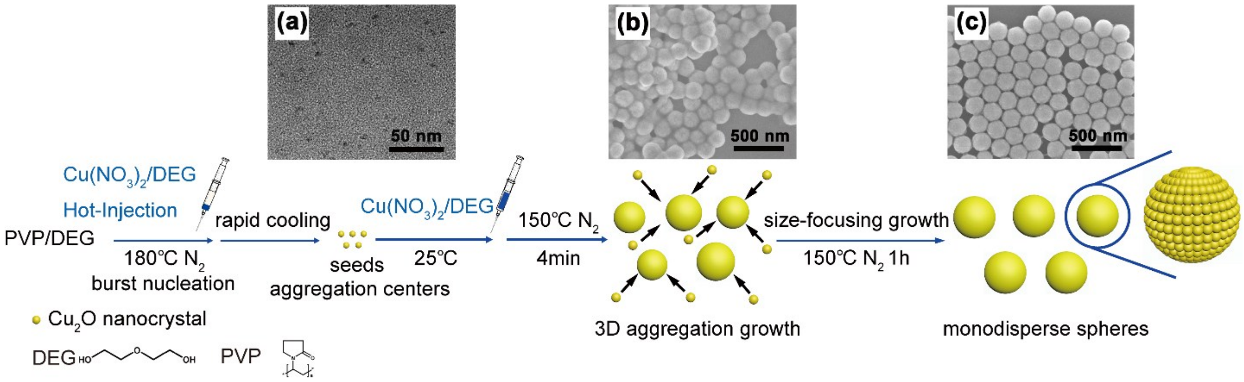

Experimental

Materials

Copper (II) nitrate trihydrate (99.5%), Cadmium (II) nitrate tetrahydrate (99%), and thiourea (99%) were all purchased from Tianjin Damao Chemical Reagents. Diethylene glycol (DEG, 98%) were purchased from Tianjin GuangFu Fine Chemical Research Institute. Poly(vinylpyrrolidone) (PVP K40, MW=40,000) were purchased from Sigma-Aldrich. All reagents were used as received without further purification.

Synthesis of monodispersed Cu_2O spheres. In a typical synthesis, 2.416 g of $Cu(NO_3)_2{\cdot}3H_2O$ was dissolved in 20 mL of DEG to make a stock solution. 1 g of PVP was dissolved in 30 mL of DEG and the solution was poured into a three-necked flask. The flask was sealed by rubber septum and heated to 180 ^oC under N_2 protection with vigorous magnetic stirring. Then 50 µL stock solutions was injected into the flask and kept at 180 ^oC for 5 min. The solution turned golden orange gradually after the injection, indicating the formation of Cu_2O seeds. The flask was then put into water bath at 25 ^oC and the solution was rapidly cooled with stirring kept. Another 1 mL of the stock solution was injected into the flask for further growth after cooling. The solution was first heated to 120 ^oC for temperature control and then slowly heated to 150 ^oC in 12 min and maintained at this temperature for 1 h. After cooling down to room temperature naturally, the products were collected by centrifugation and washed with deionized water three times and finally dispersed in ethanol for further characterization. The size of Cu_2O spheres could be facilely tuned by changing the amount of Cu precursor solution used. In a typical synthesis, 1 mL Cu precursor solution led to 187 nm Cu_2O spheres. For obtaining 93 nm, 133 nm and 165 nm Cu_2O spheres, 0.4 mL, 0.6 mL and 0.8 mL Cu precursor solution was used respectively.

Synthesis of monodispersed CdS spheres. In a typical synthesis, 6.169 g of $Cd(NO_3)_2{\cdot}4H_2O$ and 1.522 g of thiourea (TU) were dissolved respectively in 20 mL of DEG to make Cd and TU stock solution. 0.6 g of PVP was dissolved in 30 mL of DEG in advance and the solution was poured into a three-necked flask. The flask was heated to 180 ^oC with vigorous magnetic stirring. Then 100 µL of Cd and 100 µL of TU stock solution were injected into the flask continuously and kept at 180 ^oC for 5 min. The solution turned light yellow gradually after the injection indicating the formation of CdS seeds. The flask was then put into water bath at 25 ^oC and the solution was rapidly cooled with stirring kept. 0.616 g of $Cd(NO_3)_2{\cdot}4H_2O$ (2 mmol) and 0.152 g of TU (2 mmol) powder were added into the cooled solution containing seeds for further growth. Before growth reaction, the solution was first heated to 60 ^oC and kept at this temperature until all powder dissolved completely. Then the solution was heated to 160 ^oC in 16 min and maintained at this temperature for 1 h. After cooling down to room temperature naturally, the products were collected by centrifugation and washed with deionized water three times and finally dispersed in ethanol for further characterization.

Preparation of photonic crystal films. 5%wt Cu_2O ethanol dispersion were prepared with monodispersed Cu_2O spheres of 133 nm, 165 nm, and 187 nm in diameter respectively. A certain amount of Cu_2O dispersion was filled into the PMMA template and then the template was put into a vacuum drying oven at 50 ^oC for fabricating photonic crystal films. As the solvent evaporated, films with metallic lustre gradually formed.

Characterization methods

Powder X-ray diffraction (XRD) measurements were performed on a Rigaku D/MAX-2400 diffractometer with Cu-Ka radiation. The morphology of the prepared samples was investigated by Nova Nanosem 450 field emission scanning electron microscope (FE-SEM). Transmission electron microscopy (TEM), selected-area electron diffraction (SAED) and high-resolution TEM (HR-TEM) images were obtained using FEI TF30 transmission electron microscopy at 300 KV. The extinction spectra of Cu_2O spheres dispersed in ethanol was measured using a HP-8453 spectrophotometer at room temperature. Surface composition analysis of the products was performed with X-ray photoelectron spectroscopy (XPS, ESCALab 250, Thermo VG). The analysis of the spectra was based on the C 1s peak with its binding energy set as 284.6 eV.

Results and discussion

As reported in previous studies, Cu_2O colloidal spheres are polycrystalline aggregates. Their formation process was supposed to follow the "two-stage growth model" proposed by Privman and Matijevic for CdS polycrystalline spheres.[28, 31] The model involves two dynamical stages: nucleation to form nanosized primary particles (their size is usually smaller than 20 nm) and further aggregation of these primary particles into larger secondary structures (their size is usually hundreds of nanometers). In the previously reported synthesis, the two dynamical stages are occurred in one reaction system, and therefore the newly formed primary particles not only can attach to existing aggregates as basic growth units, but also serve as seeds to

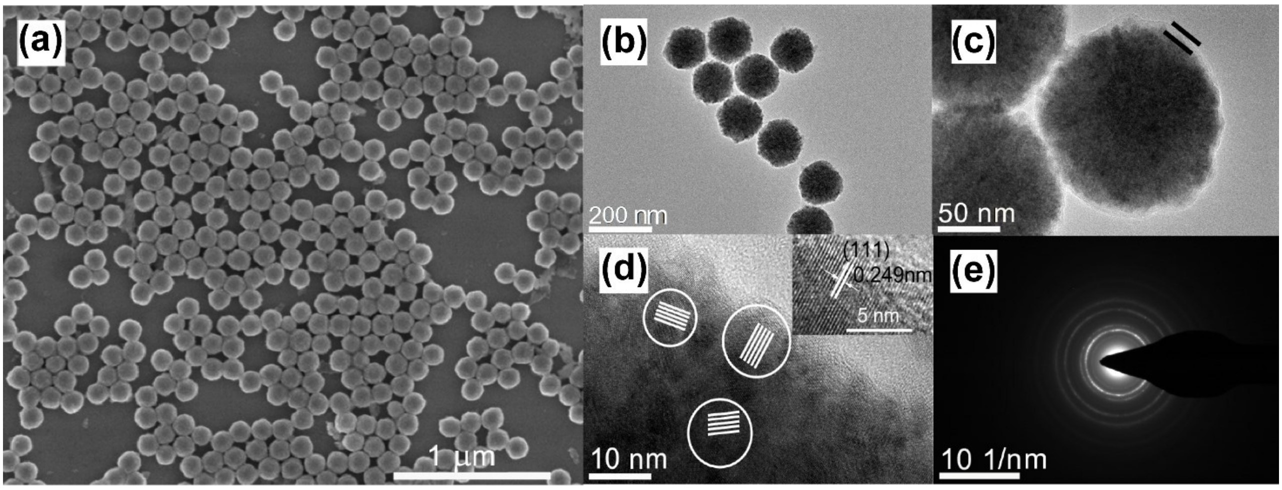

Figure 1 Images of a typical synthesis product with 0.6 mL Cu precursor added. (a)SEM image; (b-d) TEM images with different magnification times; (e) SAED image

form new aggregates. This would undoubtedly broaden the size distribution of final product due to different growth history.

According to these facts, we develop a two-step method to prepare monodispersed Cu_2O spheres using DEG as reducing agent. The key of our design is to form primary particles as seeds in the first step and make primary particles selectively attach to preformed aggregates with relatively narrow size distribution instead of forming new aggregates in the second step. As shown in Scheme 1, the whole process involves two steps which are usually called "hot-injection" and "heating-up" process. These two steps are designed based on the temperature-dependent reducing power of DEG to control the process kinetically. In the first hot-injection step at 180 ^oC, the relatively strong reducing power of DEG leads to burst nucleation of Cu_2O nanocrystals. Here, in order to avoid aggregation, limited amount of Cu precursor is added through hot-injection to create low concentration of primary particles. On the other hand, to prevent possible further aggregates formation from these particles, the reaction solution is rapidly cooled to room temperature. As shown in Scheme 1a, well-dispersed nanocrystals (primary particles) with size of 5-6 nm are obtained through the hot-injection process followed by rapid cooling. These nanocrystals can act as aggregation centers (seeds) for further growth of secondary structures in the next step. At room temperature, quantities of Cu precursor solution are added into the seeds solution for further growth. In the initial stage (150 ^oC for 4 min) of the second step, large number of primary particles are formed and attached to the surface of seeds obtained in step 1, which generate secondary aggregation structures with relatively narrow size distribution (Scheme 1b). In the further growth process, the relatively low concentration of Cu precursor remained in the solution, together with the relatively milder reducing power of DEG at 150 ^oC make the formation of primary particles in a well kinetically controllable manner, which make the newly formed primary particles selectively attach to the existing aggregates as component units rather than form new aggregates. As a result, after growing at moderate speed, the Cu_2O aggregates gradually focus into monodispersed spheres as size focusing effect (Scheme 1c).

In a typical procedure, 0.6 mL Cu precursor solution (0.5 M) was used in the heating-up process. The obtained products were characterized by field emission scanning microscopy (FE-SEM), transmission electron microscopy (TEM), selected-area electron diffraction (SAED) and high-resolution TEM (HR-TEM) (Figure 1). As seen in the Figure 1a, the obtained spheres are monodispersed with nearly identical diameter. Figure 1b further confirmed the monodispersity of the spheres. The surface of spheres is relatively rough and decorated with a thin layer of PVP, which acted as capping agent during the synthesis and providing steric repulsion to keep spheres well-dispersed in ethanol (Figure 1c, Figure S1 in the Supporting Information). Figure 1d reveals that the spheres are secondary structures which are composed of randomly oriented primary particles with size of about 10 nm. As observed in the HR-TEM image, the ordered lattice spacing is about 0.249 nm, which is close to 0.247 nm for the (111) plane of the cubic Cu_2O phase. The concentric rings pattern of SAED image (Figure 1e) clearly verified the polycrystalline nature of the spheres.

To tune the diameter of the spheres, different amounts of Cu precursor solution were added in the heating-up process. As shown in Figure 2, the diameters of Cu_2O spheres are delicately dependent on the amount of Cu precursor in the heating-up step. With the amount of Cu precursor increasing from 0.4 mL to 1 mL, diameters of the Cu_2O spheres can be precisely tuned from 93 nm to 187 nm (Figure 2a-d). The particle size distribution has been demonstrated in Figure S2 (Supporting Information) by measuring about 120 particles for each sample and the results indicate that all the products have narrow size distribution. However, the monodispersity becomes worse when 1.2 mL or more Cu precursor is added (Figure S3, Supporting Information), which make the formation of primary particles in a faster speed and lead to the aggregation growth step uncontrollable. These results indicate that it is crucial to control the concentration of Cu precursor under a certain level for obtaining monodispersed products. The phase structures of all monodispersed products are characterized by XRD. As shown in Figure 2e, all peaks are well consistent with pure cubic Cu_2O (JCPDS card number: 05-0667). The patterns are vertically offset for clarity. The primary particle sizes of the products are estimated to be around 8-9 nm by Debye-Scherrer formula according to (111) peak of the XRD patterns, which matched well with the HR-TEM image. The results reveal that the change of sphere diameter had no influence on the purity of crystalline phase and the size of primary particles remained almost the same while the size of the polycrystalline spheres increased. The size-dependent optical properties of the obtained monodispersed

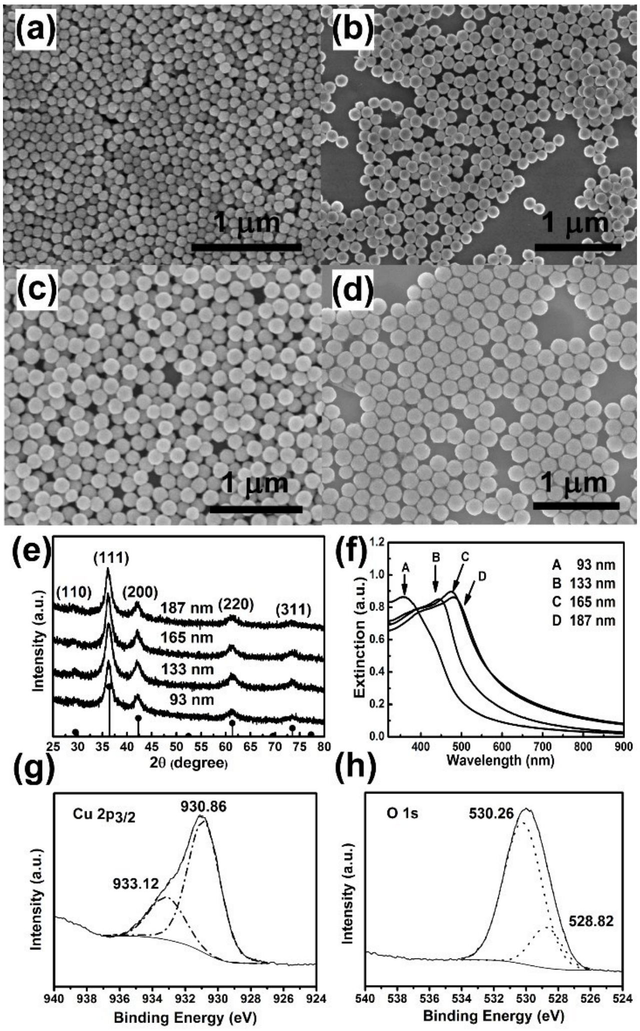

Figure 2 SEM images of Cu_2O spheres with different amount of Cu precursor. (a) 0.4 mL;(b) 0.6 mL;(c) 0.8 mL;(d) 1 mL; The diameters (a-d) are 93±7 nm, 133±10 nm, 165±10 nm, 187±13 nm respectively. (e) XRD patterns of Cu_2O products with different diameters; (f) Extinction spectra of the Cu_2O spheres in different diameters; (g-h) XPS spectrum of Cu_2O spheres in diameter of 133 nm

Cu_2O spheres are investigated by UV-vis spectroscopy. As shown in Figure 2f, the maximum absorption peaks exhibit continuous red shift as the diameter of particles increased, which is in accordance with the literature.[32] The threshold particles size for the quantum confinement effects of Cu_2O nanoparticles has been proposed to be in the range of sub-10 nm. However, the primary nanoparticle sizes of the products with different diameters are estimated to be almost same as mentioned above according to the XRD patterns and HR-TEM images. Thus, the spectral peak shift observed here is arisen from the combination of size-dependent absorbance and scattering of the spheres.

To further investigate the composition and purity of the obtained products, X-ray photoelectron spectroscopy (XPS) spectra was obtained with Cu and O as interested elements, as shown in Figure 2g, h. The Cu $2p_{3/2}$ spectrum can be resolved into two peaks: a main peak located at 930.86 eV and a small peak at 933.12 eV (Figure 2g). The main peak is ascribed to Cu^+ of Cu_2O and the small peak is attributed to Cu^{2+}, which may be CuO due to surface oxidation of Cu_2O.[27] The O 1s spectrum can be also resolved into two peaks. The main peak at 530.26 eV is attributed to Cu_2O and the small peak at 528.82 eV is ascribed to CuO. Although the presence of CuO in the product was confirmed by XPS, it was undetectable by XRD due to the tiny amount. Therefore, the high phase purity of the product was demonstrated with both the XRD and XPS results.

In the growth step, the solution color changed from transparent light green (combination effect of colors of seeds and Cu precursor) to turbid light yellow, indicating the formation of secondary structures. To investigate the growth process and the size distribution development in detail, the heating-up processes for different time were performed and the products were collected and washed by water for characterization. During the initial stage (4 min), the initial high concentration of Cu precursor makes the formation of primary particles and the further aggregation behavior of them rather rapid, which results in irregular shapes of these secondary structures (Figure S4a). Due to the presence of preformed seeds, the size distribution of these secondary structures is controlled to be relatively narrow and this is the prerequisite for obtaining monodispersed products. As Cu precursor has been extensively consumed, the formation of primary particles in the remaining growth process can be controlled in a moderate rate. Newly formed primary particles selectively attach on the surface of preformed secondary structures to form spheres with narrow size distribution gradually and maintained the monodispersity

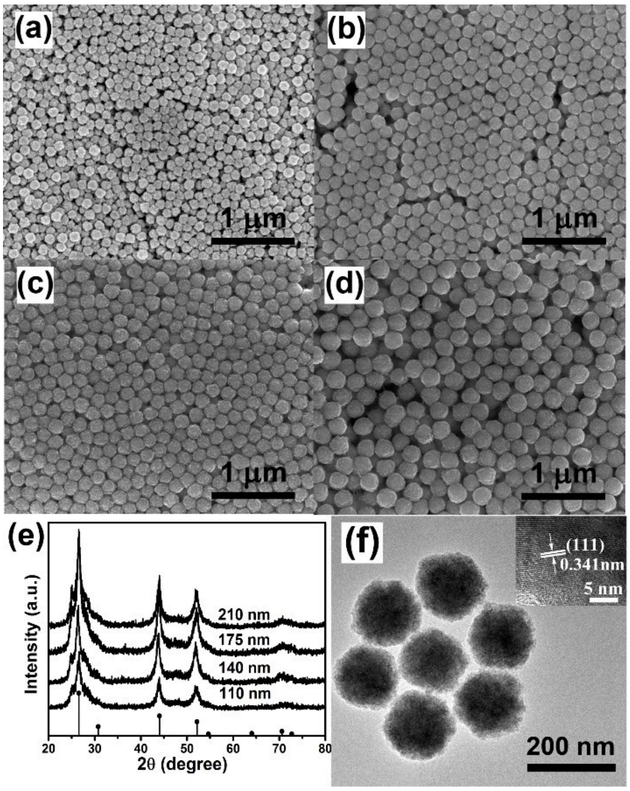

Figure 3 (a-d) SEM images of CdS spheres with different amount of Cd precursor for further growth.(a) 2 mmol,110 nm;(b) 4 mmol,140 nm;(c) 5 mmol,175 nm;(d) 6 mmol,210 nm; The molar ratio of Cd and TU was kept 1:1 in all experiments;(e) XRD patterns of CdS products with different diameters;(f) TEM image of typical products(inset: HR-TEM image of a CdS sphere showing the nanocrystalline domains)

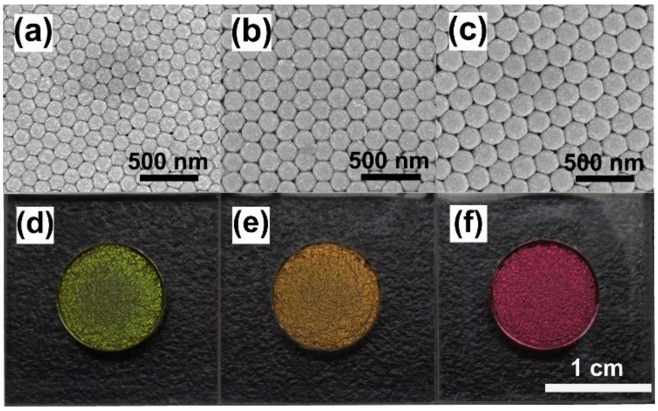

Figure 4. SEM images of photonic crystal films with Cu_2O spheres in different diameters as building blocks: (a) 133 nm; (b) 165 nm;(c) 187 nm; (d-f) digital photograph of Cu_2O photonic crystal films fabricated in PMMA template with Cu_2O spheres in diameter of 133 nm, 165 nm and 187 nm respectively.

with diameter slightly increased (Figure S4b, c). The results are somewhat like the "size-focusing effect" that smaller particles grow faster than larger ones to make the size distribution focusing.[33] The key point of our "size-focusing" herein is to make the reaction proceed in a moderate speed, which is closely related to the temperature-dependent reducing power of DEG. As a control experiment, we conducted the heating-up process at a higher temperature (160 °C) and the morphology of as obtained products is shown in Figure S4d. It is obvious that the higher temperature results in the Cu_2O spheres with poor size distribution owing to more rapid growth rate in higher temperature. Hence an appropriate growth speed in the growth stage is important for achieving monodisperse Cu_2O spheres.

To confirm the necessity of seeds in the solution before further growth, reactions under different heating rates from 120 °C to 150 °C without seeds are carried out because heating rates have great impact on particle size and size distribution. As shown in Figure S5 (Supporting Information), all products are not uniform in size under any heating rates, which includes the heating rate as same as the typical synthesis (Figure S5b). Without the preformed seed, primary particles aggregate spontaneously and growth centers are continued to be generated by precursor for further growth, which lead to different growth history of secondary structures and thus poor size distribution. The results highlight that the presence of seeds is necessary for preparing monodisperse Cu_2O spheres. In one word, three key factors in the method determined the narrow size distribution of Cu_2O spheres: burst nucleation at higher temperature and rapid cooling to form seeds during hot-injection step, proper amount of Cu precursor during the heating-up step, and moderate reaction rate at certain temperature during the heating-up step.

Based on the developed method described above, monodisperse CdS spheres with diameters in the range from 110 nm to 210 nm were also prepared by simply changing the amount of Cd precursor for further growth. As shown in Figure 3a-d, all products are of good monodispersity and uniform morphology. The structures of all monodispersed products were characterized by XRD, with all peaks indexed as pure cubic CdS (JCPDS card number: 08-0019) as shown in Figure 3e. The spectra were vertically offset for clarity. TEM image further confirmed the monodispersity of the products (Figure 3f). As observed in the high-resolution transmission electron microscopy (HR-TEM) image, the ordered lattice spacing is about 0.341 nm, which is close to 0.336 nm for the (111) plane of the cubic CdS phase.

Finally, with the obtained monodisperse Cu_2O spheres as building blocks, photonic crystal films with brilliant and saturated structural color are fabricated through an evaporated-induced self-assembly process. As the solvent evaporates, monodispersed spheres spontaneously self-assemble into highly ordered arrays with (111) plane parallel to the substrate as shown in Figure 4a-c. The brilliant and saturated structural color of the Cu_2O photonic crystal proves the existence of its strong band gap (Figure 4d-f).

Conclusions

In summary, we have developed a novel two-step method to prepare monodispersed Cu_2O spheres. The method involved a hot-injection step for seeds preparation and a heating-up step for further growth. The temperature-dependent reducing power of DEG made the reaction process kinetically controllable and well reproducible. The key points of the method including the essential presence of seeds before further growth, proper precursor concentration level, and moderate growth speed were investigated carefully and demonstrated. Based on the developed method, monodispersed CdS spheres with diameters in the range from 110 nm to 210 nm were also prepared and it was expected that this method could be extended to other spherical polycrystalline aggregation with high refractive index. Photonic crystal films with brilliant structural color were fabricated by assembling monodisperse Cu_2O spheres into ordered photonic crystal structures. Our results demonstrate the success in achieving colloidal spheres of high refractive index materials with narrow size distribution and controllable size and provide the possibility to build photonic crystal possessing brilliant structural color (strong band gap).

Acknowledgements

This work was supported by the National Natural Science Foundation of China (21476040, 21276040), China Postdoctoral Science Foundation (2013M530921), China Postdoctoral Science Special Foundation (2014T70241), Fund for innovative research groups of the National Natural Science Fund Committee of Science (21421005), Innovation team of Ministry of Education (IRT-13R06), Innovation team of Dalian University of Technology (DUT2013TB07).

Notes and references

1. D. J. Norris and Y. A. Vlasov, *Adv. Mater.*, 2001, **13**, 371-376.
2. D. P. Josephson, E. J. Popczun and A. Stein, *The Journal of Physical Chemistry C*, 2013, **117**, 13585-13592.
3. C. C. Li, Y. P. Zheng and T. H. Wang, *J. Mater. Chem.*, 2012, **22**, 13216-13222.

4. D. P. Josephson, M. Miller and A. Stein, *Z. Anorg. Allg. Chem.*, 2014, **640**, 655-662.
5. G. von Freymann, V. Kitaev, B. V. Lotsch and G. A. Ozin, *Chem. Soc. Rev.*, 2013, **42**, 2528-2554.
6. J. F. Galisteo-López, M. Ibisate, R. Sapienza, L. S. Froufe-Pérez, Á. Blanco and C. López, *Adv. Mater.*, 2011, **23**, 30-69.
7. M. G. Han, C. G. Shin, S.-J. Jeon, H. Shim, C.-J. Heo, H. Jin, J. W. Kim and S. Lee, *Adv. Mater.*, 2012, **24**, 6438-6444.
8. A. Stein, B. E. Wilson and S. G. Rudisill, *Chem. Soc. Rev.*, 2013, **42**, 2763-2803.
9. E. W. Seelig, B. Tang, A. Yamilov, H. Cao and R. P. H. Chang, *Mater. Chem. Phys.*, 2003, **80**, 257-263.
10. X. Hu, J. Gong, L. Zhang and J. C. Yu, *Adv. Mater.*, 2008, **20**, 4845-4850.
11. X.-H. Li, J.-X. Li, G.-D. Li, D.-P. Liu and J.-S. Chen, *Chemistry – A European Journal*, 2007, **13**, 8754-8761.
12. K. P. Velikov and A. van Blaaderen, *Langmuir*, 2001, **17**, 4779-4786.
13. V. Ladmiral, T. Morinaga, K. Ohno, T. Fukuda and Y. Tsujii, *Eur. Polym. J.*, 2009, **45**, 2788-2796.
14. Y. Wang, L. Cai and Y. Xia, *Adv. Mater.*, 2005, **17**, 473-477.
15. U. Jeong and Y. Xia, *Adv. Mater.*, 2005, **17**, 102-106.
16. L. Liu, Q. Peng and Y. Li, *Nano Research*, 2008, **1**, 403-411.
17. X. Jiang, T. Herricks and Y. Xia, *Adv. Mater.*, 2003, **15**, 1205-1209.
18. S. Liu, G. Han, M. Shu, L. Han and S. Che, *J. Mater. Chem.*, 2010, **20**, 10001-10009.
19. A. T. Marin, D. Muñoz-Rojas, D. C. Iza, T. Gershon, K. P. Musselman and J. L. MacManus-Driscoll, *Adv. Funct. Mater.*, 2013, **23**, 3413-3419.
20. A. Goyal, A. L. M. Reddy and P. M. Ajayan, *Small*, 2011, **7**, 1709-1713.
21. L. Hu, Y. Huang, F. Zhang and Q. Chen, *Nanoscale*, 2013, **5**, 4186-4190.
22. Z. Zhang, R. Dua, L. Zhang, H. Zhu, H. Zhang and P. Wang, *ACS Nano*, 2013, **7**, 1709-1717.
23. K. Chen, C. Sun and D. Xue, *PCCP*, 2015, **17**, 732-750.
24. K. Chen, C. Sun, S. Song and D. Xue, *CrystEngComm*, 2014, **16**, 5257-5267.
25. K. Chen and D. Xue, *Nanoscience and Nanotechnology Letters*, 2011, **3**, 383-388.
26. X. Zhao, Z. Bao, C. Sun and D. Xue, *J. Cryst. Growth*, 2009, **311**, 711-715.
27. M. Pang and H. C. Zeng, *Langmuir*, 2010, **26**, 5963-5970.
28. L. Zhang and H. Wang, *ACS Nano*, 2011, **5**, 3257-3267.
29. J. Zhang, J. Liu, Q. Peng, X. Wang and Y. Li, *Chem. Mater.*, 2006, **18**, 867-871.
30. B. Wiley, Y. Sun, B. Mayers and Y. Xia, *Chemistry – A European Journal*, 2005, **11**, 454-463.
31. S. Libert, V. Gorshkov, D. Goia, E. Matijević and V. Privman, *Langmuir*, 2003, **19**, 10679-10683.
32. R. Bardhan, N. K. Grady, T. Ali and N. J. Halas, *ACS Nano*, 2010, **4**, 6169-6179.
33. X. Peng, J. Wickham and A. P. Alivisatos, *J. Am. Chem. Soc.*, 1998, **120**, 5343-5344.